Available online at www.sciencedirect.com
SCIENCE DIRECT
Catalysis Today 111 (2006) 333–337
CATALYSIS TODAY
www.elsevier.com/locate/cattod

A theoretical study on Brønsted acidity of WO_3 clusters supported on metal oxide supports by "paired interacting orbitals" (PIO) analysis

A. Shiga [a,*], N. Katada [b], M. Niwa [b]

[a] *LUMMOX Reseach Laboratory, Takezono 2-18-4-302, Tsukuba 305-0032, Japan*
[b] *Department of Materials Science, Faculty of Engineering, Tottori University, Koyama, Tottori 680-8552, Japan*

Abstract

Ammonia adsorption on Brønsted acid sites of WO_3 cluster supported on metal oxide supports: SnO_2, ZrO_2, and TiO_2, is analyzed by PIO analysis. We employed $(HO)(WO_3)_4(H)$ and $(HO)(WO_3)_9(H)$ on $(SnO_2)_{12}$, $(ZrO_2)_{12}$, and $(TiO_2)_{12}$, respectively, as supported Brønsted acid models and examined two types of Brønsted acid sites, an edge type and a face type. We estimated ammonia adsorption strength by total overlap population ($\sum$OP) of all PIOs between the Brønsted acid site and NH_3. The order of acidity ($\sum$OP) of each model is as follows: edge type: SnO_2, $0.0096 > ZrO_2$, $0.0048 > TiO_2$, $-0.0001 \gg$ face type: ZrO_2, $-0.0759 > TiO_2$, $-0.0761 > SnO_2$, -0.0867. The edge type adsorption is far stronger than the face type one. This order in the edge type coincides with the experimental results. The reason of these results is explained by the difference of the influence of oxygen atoms sitting near the N atom of NH_3.

Keywords: WO_3 cluster; Metal oxide supports; SnO_2; ZrO_2; TiO_2; Brønsted acidity; NH_3 adsorption; Interacting orbital analysis

1. Introduction

It is already reported that such metal oxides as MoO_3, WO_3, and V_2O_5 spread readily on supports like SnO_2, ZrO_2, and TiO_2, generate Brønsted acid sites on the metal oxide monolayer cluster which contain four to eight metal atoms, and sequence of the metal oxide to show the strong acidity is, $WO_3 > MoO_3 > V_2O_5$, and for the support oxide to accommodate the monolayer, $SnO_2 > ZrO_2 > TiO_2$ [1]. In this paper, we study the NH_3 adsorption on the monolayer WO_3 supported on SnO_2, ZrO_2, and TiO_2 to clarify the roles of the supports by using paired interacting orbitals (PIO) analysis proposed by Fujimoto et al. [2].

2. Models and calculation methods

2.1. Models

We employed $(HO)(WO_3)_4(H)$ and $(HO)(WO_3)_9(H)$ clusters supported on metal oxide clusters, $(SnO_2)_{12}$, $(ZrO_2)_{12}$, and $(TiO_2)_{12}$, respectively. Structural parameters of the WO_3 clusters and support metal oxides were referred from ICSD data base [3]. We generated Brønsted acid site by adding $(H)^+$ and $(OH)^-$ ions on WO_3 clusters and coordinated NH_3 molecule to the acid site. Referring also structural parameters of titanium oxide from ICSD data base we construct artificial single layered support metal oxides having the distance d(W, Sn, Ti, Zr–O) = 2.000 Å, and the angle $\angle$WOSn, Ti, Zr = 90.0°, $\angle$SnOSn, TiOTi, ZrOZr = 90.0°. Another structural parameters, which we assumed, are shown as follows: the distance d(O–H) of B-acid = 0.957 Å, d(W–terminal O) = 1.800 Å, d(H of B-site between N) = 2.500 Å, 1.844 Å, and the angle $\angle$WOH = 105.0°, Turning the direction of O–H from 3:00(**0 0**) to 1:30(**0 1**), 12:00(**0 2**), 10:30(**0 3**) until to 9:00(**0 4**) in the x–y plane, anti-clock wisely, and comparing the two approaching directions of NH_3 along x-axis or z-axis, we explored the position of NH_3 coordination. We examined two types of Brønsted acid sites, an edge type and a face type, shown in Fig. 1.

2.2. PIO calculation

The PIO analysis is a method for unequivocally determining the orbitals which should play dominant roles in chemical interactions between two systems, [A] and [B], which are constructing a combined system [C]. Here, [A] is supported

* Corresponding author.
E-mail address: aas55@mail2.accsnet.ne.jp (A. Shiga).

0920-5861/$ – see front matter © 2005 Elsevier B.V. All rights reserved.
doi:10.1016/j.cattod.2005.10.059

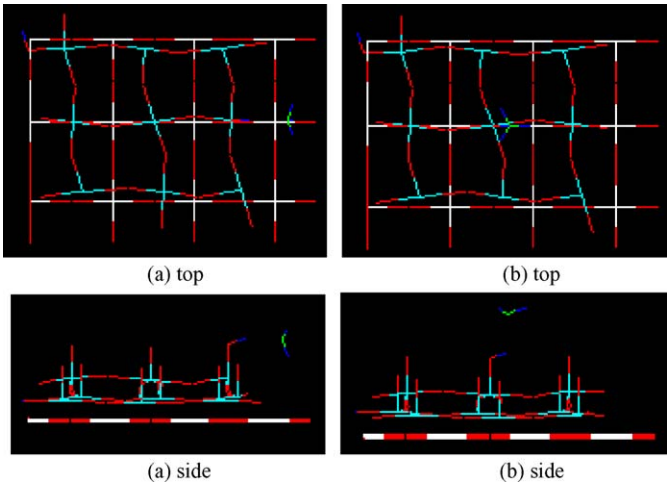

Fig. 1. Top and side views of NH_3 coordination on $(HO)(WO_3)_{4,9}(H)/(SnO_2)_{12}$: (a) edge type and (b) face type.

WO_3 moiety and [B] is NH_3. The geometries of [A] and [B] are the same as those in the complex [C] ([A–B] ≡ [C]).

The MOs of [A], [B], and [C] were calculated by the extended Hückel method and the PIOs were obtained according to the procedure developed by Fujimoto et al. [2]. We used EH parameters reported by Herman [4]. They are shown in Appendix A.

(1) The MOs of a complex are expanded in terms of the MOs of two fragment species, to determine the expansion coefficients $c_{i,f}$, $c_{m+j,f}$, $d_{k,f}$, and $d_{n+l,f}$ in Eq. (1)

$$\Phi_f = \sum_{i=1}^{m} c_{i,f}\phi_i + \sum_{j=1}^{M-m} c_{m+j,f}\phi_{m+j} + \sum_{k=1}^{n} d_{k,f}\psi_k + \sum_{l=1}^{N-n} d_{n+1,f}\psi_{n+l}, \quad f = 1, 2, \ldots, m+n, \tag{1}$$

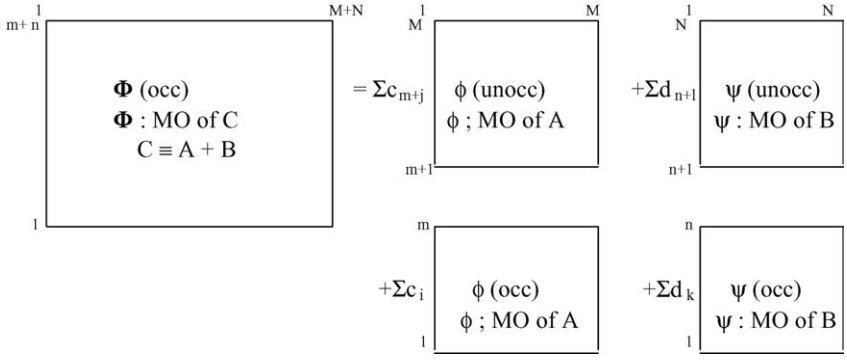

(2) An interaction matrix P is constructed which represents the interaction between the MOs of the fragment [A] and the MOs of the fragment [B]

$$P = \begin{pmatrix} p_{i,k} & p_{i,n+l} \\ p_{m+j,k} & p_{m+j,n+l} \end{pmatrix} \tag{2}$$

in which

$$p_{i,k} = n_{t,u}\sum_{f=1}^{m+n} c_{i,f}d_{k,f}, \quad i = 1-m, \quad k = 1-n$$

$$p_{i,n+l} = n_{t,u}\sum_{f=1}^{m+n} c_{i,f}d_{n+l,f}, \quad i = 1-m, \quad l = 1-(N-n)$$

$$p_{m+j,k} = n_{t,u}\sum_{f=1}^{m+n} c_{m+j,f}d_{k,f}, \quad j = 1-(M-m), \quad k = 1-n$$

$$p_{m+j,n+l} = n_{t,u}\sum_{f=1}^{m+n} c_{m+j,f}d_{n+l,f}, \quad j = 1-(M-m), \quad l = 1-(N-n)$$

(3) Transformation matrices U^A (for A) and U^B (for B) are obtained by

$$\tilde{P}PU^A = U^A\Gamma \tag{3}$$

$$(PU^A)(PU^A) = \Gamma \tag{4}$$

$$U^{B_{s,v}} = (\gamma_v)^{-1/2}\sum_{r}^{N} p_{r,s}U^{A_{r,v}}, \quad v = 1, 2, \ldots, N, \tag{5}$$

where the diagonal element of Γ, which is γ_v ($v = 1, \ldots, N$), means the square of interaction strength.

Finally the PIOs are obtained by Eqs. (6) and (7)

$$\phi'_v = \sum_{r}^{N} UU^{A_{r,v}}\phi_r \quad (\text{for A}) \tag{6}$$

$$\psi'_v = \sum_{s}^{N} U^{B_{s,v}}\psi_s \quad (\text{for B}). \tag{7}$$

The $N \times M$ ($N < M$) orbital interactions in the complex C can thus be reduced to the interactions of N PIOs, where N indicating smaller numbers of MOs of the two fragments, A and B. Although this analysis was proposed originally for ab initio calculations, we reported that this approach was useful also in analyzing the results of extended Hückel MO calcula-

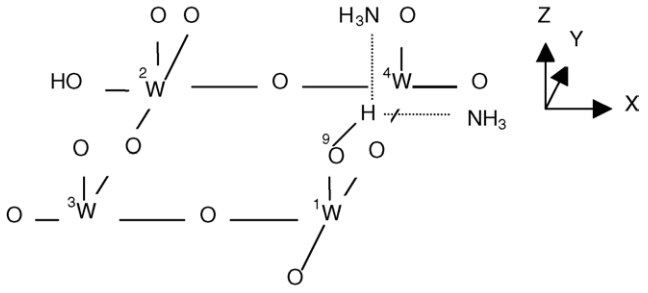

Fig. 2. A schematic illustration of NH_3 coordination on $(HO)(WO_3)_4(H)$.

tions [5–7]. PIO calculations were carried out on *LUMMOX*™ system [8,9].

3. Investigation of the positions of NH_3 coordinated to B-acid site

We employed $(HO)(WO_3)_4(H)$ cluster and explored five positions of NH_3 around W=O axis, 3:00 o'clock: (0 0), 1:30 o'clock: (0 1), 12:00 o'clock: (0 2), 10:30 o'clock: (0 3), 9:00 o'clock: (0 4), and another two positions from *z*-axis, (0 0 *z*) and (0 3 *z*). They are shown in Fig. 2.

Total energies (E_c) of NH_3 coordination on $(HO)W_4O_{12}(H)$ are summarized in Table 1. Table 1 tells us that the position of (**0 2**) and (**0 4**) are very unstable and the coordination from *z*-axis is unfavorable. Using PIO analysis, we examined (0 0), (0 3), (0 0 *z*), and (0 3 *z*), precisely.

The eigen values of PIOs of NH_3 coordination on $(HO)(WO_3)_4(H)$ are shown in Table 2. An eigen value of PIO means the contribution of the PIO to the interaction. Table 2 tells us that the interaction between NH_3 and $(HO)(WO_3)_4(H)$ is expressed by one major interaction, PIO-1, and two relatively minor interactions, PIO-2 and PIO-3. The contour maps of these three PIOs: PIO-1, PIO-2, and PIO-3 of each model are shown in Fig. 3. In the case of model (**0 0**), the PIO-1 represents an in-phase interaction between the hydrogen of B-acid and the N atom of the NH_3, that is the origin of ammonia coordination, the PIO-2 represents an out of phase (that is repulsive) interaction between the O atom of B-acid and the N atom of the NH_3, and the PIO-3 represents also an out of phase interaction between the O atoms near by B-acid site and the N atom of the NH_3. On the other hand, in the case of model (**0 3**), and (**0 0** ***z***), PIO-1, the most important PIO, represents a large out of phase interaction between the O atom of B-acid and the N atom of the NH_3.

Table 1
Total energies (E_c) of NH_3 coordination on $(HO)W_4O_{12}(H)$

Sample states	E_c (eV)	ΔE (eV)
OH···NH_3 distance 1.844 Å		
(**0 0**)	−2025.74	0.0
(**0 1**)	−2026.11	−0.37
(**0 2**)	−2020.58	+5.16
(**0 3**)	−2025.57	+0.17
(**0 4**)	−2015.41	+10.33
(**0 0** *z*)	−2024.91	+0.83
(**0 3** *z*)	−2025.01	+0.73

$\Delta E = E_c$ (each state) − E_c (0 0).

The overlap population of each PIO and the sum of all PIOs ($\sum$OP) are shown in Table 3. The $\sum$OP of each model is almost the same value as the sum of overlap populations of those major contributed three PIOs. We use the $\sum$OP as an indicator of the strength of NH_3 coordination. The larger the $\sum$OP value, the more favorably the NH_3 coordination takes place. From the $\sum$OP value, we can estimate that the edge type model (**0 0**) is favorable for ammonia coordination to B-acid of WO_3 cluster.

4. NH_3 coordination to B-acid site of $(HO)(WO_3)_9(H)$ cluster supported on metal oxides

Here, we employed $(HO)(WO_3)_9(H)$ cluster supported on metal oxides, $(SnO_2)_{12}$, $(ZrO_2)_{12}$, and $(TiO_2)_{12}$, respectively.

Table 2
Eigen values of each PIOs of ammonia coordination on $[(OH)(WO_3)_4(H)]$

Model	PIO-1	PIO-2	PIO-3	PIO-4	PIO-5	PIO-6	PIO-7
R = 1.844 Å							
(**0 0**)	**0.0949**	**0.0181**	**0.0020**	0.0003	0.0002	0.0000	0.0000
(**0 3**)	**0.1190**	**0.0744**	**0.0563**	0.0237	0.0046	0.0029	0.0014
(**0 0** *z*)	**0.1516**	**0.0197**	**0.0071**	0.0012	0.0005	0.0001	0.0000
(**0 3** *z*)	**0.1427**	**0.0131**	**0.0049**	0.0026	0.0004	0.0001	0.0000

Table 3
Overlap populations of each PIOs of ammonia coordination on $[(OH)(WO_3)_4(H)]$

Model	PIO-1	PIO-2	PIO-3	PIO-4	PIO-5	PIO-6	PIO-7	$\sum$OP
R = 1.844 Å								
(**0 0**)	**0.0433**	**−0.0318**	**0.0055**	0.0005	0.0015	−0.0004	0.0000	**0.0186**
(**0 3**)	**−0.0795**	**0.0103**	**−0.0258**	−0.0120	0.0033	−0.0018	0.0011	**−0.1044**
(**0 0** *z*)	**−0.0587**	**−0.0116**	**0.0010**	−0.0009	0.0019	0.0002	0.0000	**−0.0681**
(**0 3** *z*)	**−0.0667**	**−0.0082**	**0.0008**	−0.0010	0.0012	0.0003	0.0001	**−0.0735**

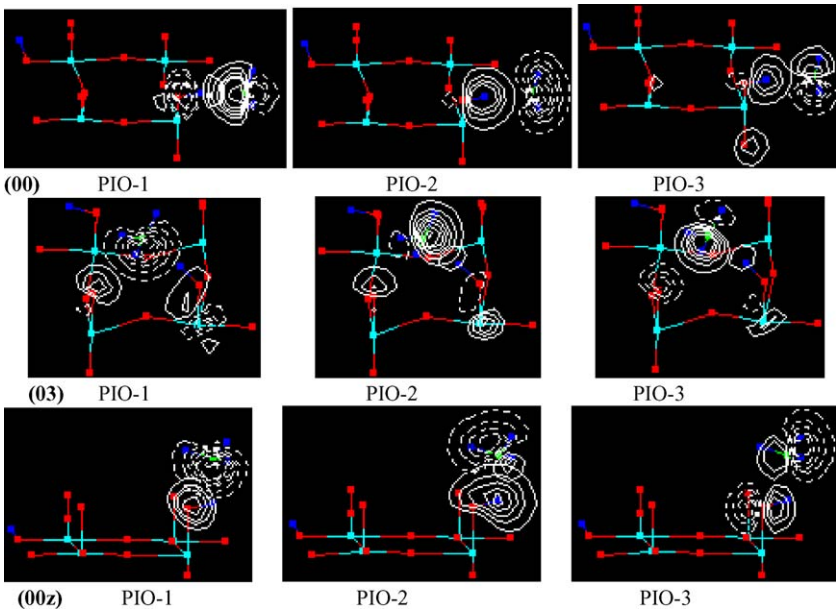

Fig. 3. Contour maps of PIO-1, PIO-2, and PIO-3 of model (**0 0**), (**0 3**), and (**0 0** *z*).

Calculation results are summarized in Table 4. As the differences of the ΔE are very small, it is difficult to estimate the NH_3 adsorption strength by the ΔE. On the other hand, we can estimate NH_3 adsorption strength by total overlap population ($\sum$OP) of all PIOs. The order of $\sum$OP of each model is as follows: edge type: SnO_2, $0.0096 > ZrO_2$, $0.0048 > TiO_2$, $-0.0001 \gg$ face type: ZrO_2, $-0.0759 > TiO_2$, $-0.0761 > SnO_2$, -0.0867. The edge type adsorption is far stronger than the face type one. The reason is that since the distance between the N atom and the O atom of B-acid is shorter in the case of face type than that in the case of edge type, the repulsive out of phase interaction is larger in the case of face type adsorption. The influence of the support oxides on NH_3 adsorption is clearly expressed in the value of $\sum$OP. The repulsive effect of the O atom of support oxides, which is situated below the W atom and trans position of the B-acid of WO_3, increases by the extent of d orbital interaction of the metal of support oxides. The order in the edge type adsorption coincides with the experimental results. The $\sum$OP of the NH_3 adsorption to the corner type B-acid of $(HO)(WO_3)_4(H)$ cluster on metal oxides is larger than that of the edge type one of $(HO)(WO_3)_9(H)$ cluster on each corresponding metal oxide. The reason is based on the difference of the cluster size, the number of WO_3 unit, 4 and 9. Recently, Satsuma et al. reported that WO_3 layered clusters containing three to five W atoms were observed on the surface of ZrO_2 particles by high resolution TEM [10]. In the case of $(HO)(WO_3)_4(H)$ cluster all B-acid sites are corner type.

From these results, it is suggested that one of the important roles of support oxides is to generate and to stabilize this small $(HO)(WO_3)_4(H)$ cluster on them.

Table 4
Total energies (E_c), ΔE and total overlap population ($\sum$OP) of NH_3 coordination on $(HO)(WO_3)_{4,9}(H)/(SnO_2)_{12}$, $(TiO_2)_{12}$, and $(ZrO_2)_{12}$

Models	E_c (eV)	ΔE (eV)	$\sum$OP
Edge type: edge OH···NH_3 distance 1.844 Å, *x*-axis ^{6}W: five-fold coordination			
$(HO)(WO_3)_9(H)\_(SnO_2)_{12}\_(NH_3)$ (**0 0**)	−7600.57	+0.02	0.0096
$(HO)(WO_3)_9(H)\_(ZrO_2)_{12}\_(NH_3)$ (**0 0**)	−7596.84	−0.01	0.0048
$(HO)(WO_3)_9(H)\_(TiO_2)_{12}\_(NH_3)$ (**0 0**)	−7588.40	−0.02	−0.0001
Face type: face OH···NH_3 distance 1.844 Å, *z*-axis ^{5}W: six-fold coordination			
$(HO)(WO_3)_9(H)\_(SnO_2)_{12}\_(NH_3)$ (**0 0** *z*)	−7602.76	+0.92	−0.0867
$(HO)(WO_3)_9(H)\_(ZrO_2)_{12}\_(NH_3)$ (**0 0** *z*)	−7598.98	+0.87	−0.0759
$(HO)(WO_3)_9(H)\_(TiO_2)_{12}\_(NH_3)$ (**0 0** *z*)	−7590.22	+0.86	−0.0761
Corner type: corner OH···NH_3 distance 1.844 Å, *x*-axis ^{1}W: five-fold coordination			
$(HO)(WO_3)_4(H)\_(SnO_2)_{12}\_(NH_3)$ (**0 0**)	−5452.29	+0.04	0.0099
$(HO)(WO_3)_4(H)\_(ZrO_2)_{12}\_(NH_3)$ (**0 0**)	−5426.75	−0.04	0.0107
$(HO)(WO_3)_4(H)\_(TiO_2)_{12}\_(NH_3)$ (**0 0**)	−5413.20	−0.04	0.0044

$\Delta E = E_c - (E_a + E_b)$, E_a is the energy of the fragment A, that is catalyst portion, and E_b is the energy of the fragment B, that is ammonia.

5. Conclusion

Ammonia adsorption on Brønsted acid sites of WO_3 cluster supported on metal oxide supports: SnO_2, ZrO_2, and TiO_2, is studied by PIO analysis. Conclusions are the following:

(1) the edge type B-acid is far stronger than the face type one;
(2) the influence of the support oxides is properly estimated by the $\sum$OP value;
(3) the size and shape of WO_3 cluster supported on metal oxides is a layered WO_3 tetramer;
(4) important role of support oxides is to stabilize this layered $(HO)(WO_3)_4(H)$ cluster on them;
(5) finally, the PIO analysis based on EHMO is a useful way for understanding reaction mechanisms, especially in large catalytic systems.

Appendix A

Coulomb integrals and orbital exponents are listed in Table A.1.

Table A.1
Extended Hückel parameters

Orbital	Hii (eV)	ζ_1
H 1s	−13.598	1.000
N 2s	−26.685	2.0348
N 2p	−14.534	1.9398
O 2s	−28.541	2.2399
O 2p	−13.618	2.0477
Ti 4s	−6.828	1.3416
Ti 4p	−3.973	1.0104
Ti 3d	−10.495	2.6439
Zr 5s	−6.634	1.350
Zr 5p	−3.866	1.350
Zr 4d	−8.740	2.3831
Sn 5s	−14.519	2.4041
Sn 5p	−7.344	1.9128
W 6s	−7.864	1.800
W 6p	−4.375	1.800
W 5d	−12.293	3.1936

References

[1] Y. Habuta, N. Narishige, K. Okumura, N. Katada, M. Niwa, Catal. Today 78 (2003) 131.
[2] H. Fujimoto, T. Yamasaki, H. Mizutani, Koga, J. Am. Chem. Soc. 107 (1986) 6157.
[3] WO_3: E. Gebert, R.J. Ackermann, Inorg. Chem. 5 (1996) 136; TiO_2: R. Restori, D. Schwarzenbach, J.R. Schneider, Acta Crystallographica, Section B 43B (1987) 251.
[4] A. Herman, Modell. Simul. Sci. Eng. 12 (2004) 21.
[5] A. Shiga, J. Kojima, T. Sasaki, Y. Kikuzono, J. Organomet. Chem. 345 (1988) 275.
[6] A. Shiga, H. Kawamura, T. Ebara, T. Sasaki, Y. Kikuzono, J. Organomet. Chem. 366 (1989) 95.
[7] A. Shiga, J. Mol. Catal. A 146 (1999) 325.
[8] H. Katsumi, Y. Kikuzono, M. Yoshida, A. Shiga, H. Fujimoto, LUMMOX, Sumitomo Chemical Co. Ltd., Tokyo, 1999.
[9] T. Motoki, A. Shiga, J. Comput. Chem. 25 (2004) 106.
[10] A. Satsuma, H. Yokoi, H. Nishiyama, S. Kakimoto, S. Sugaya, T. Oshima, T. Hattori, Chem. Lett. 33 (2004) 1250.